

Micromechanical failure analysis of composite materials subjected to biaxial and off-axis loading

Isa Ahmadi*

*Advanced Materials and Computational Mechanics Lab., Department of Mechanical Engineering,
University of Zanjan, University Blvd, 45371-38791, Zanjan, Iran*

(Received April 6, 2016, Revised November 24, 2016, Accepted December 28, 2016)

Abstract. In this study, the failure behavior of composite material in the biaxial and off-axis loading is studied based on a computational micromechanical model. The model is developed so that the combination of mechanical and thermal loading conditions can be considered in the analysis. The modified generalized plane strain assumption of the theory of elasticity is used for formulation of the micromechanical modeling of the problem. A truly meshless method is employed to solve the governing equation and predict the distribution of micro-stresses in the selected RVE of composite. The fiber matrix interface is assumed to be perfect until the interface failure occurs. The biaxial and off-axis loading of the SiC/Ti and Kevlar/Epoxy composite is studied. The failure envelopes of SiC/Ti and Kevlar/Epoxy composite in off-axis loading, biaxial transverse-transverse and axial-transverse loading are predicted based on the micromechanical approach. Various failure criteria are considered for fiber, matrix and fiber-matrix interface. Comparison of results with the available results in the literature shows excellent agreement with experimental studies.

Keywords: micromechanics of failure; off-axis loading; biaxial loading; meshless methods; failure envelope

1. Introduction

The properties of metal-matrix composites (MMCs) exceptionally good stiffness-to-weight and strength-to-weight ratio and high temperature resistance make it attractive in many structural applications especially in weight-sensitive components at high temperature applications, such as applications in aerospace, gas turbine engines and other structural components. Unidirectional metal matrix composites have their best performance in the direction of the fibers, but in the most applications these materials are subjected to loads that are not in the fiber or normal to the fiber direction. This type of loading is usually called off-axis loading. In addition, due to mismatch in the thermo-mechanical properties of fibers and matrix thermal residual stresses arise in the manufacturing process of metal matrix composite and the presence, the sign, and the magnitude of the residual stresses significantly affect the yield strength, and the fracture toughness of the resulting MMCs.

Off-axis loading of composite materials has been studied theoretically at both macro- and micro-mechanical view. At a macro-mechanical view the composite is presumed to be a material which is macroscopically homogeneous and has orthotropic properties. A number of continuum models have been proposed to predict the behavior of composite materials subjected to off-axis loading. Among the earliest efforts to study the off-axis

behavior of composite materials are the analytical and experimental studies carried out by Jackson and Cratchley (1996), Cooper (1996), Pipes and Cole (1973).

At the micromechanical view, the composite is treated as a heterogeneous material consisting of fibers embedded in the matrix. Many attempts have been made to develop micromechanical models to predict the behavior of composite subjected to various types of loading. Most of these studies are limited to the application of normal loading in the transverse and axial directions (Adams 1970, Dvorak *et al.* 1973, Nimmer 1990, Wisnom 1990, Zahl *et al.* 1994, Li and Wisnom 1996, Nimmer *et al.* 1991, Aghdam *et al.* 2000). Some other studies have considered shear loading in the micromechanical modeling of the composites (Adams and Doner 1967, Adams and Crane 1984a, b, Brockenbrough *et al.* 1991, Naik and Crews 1993, Sun and Vaidya 1996, Dang and Sankar 2008, Ahmadi and Aghdam 2010a). Adams and Crane (1984a, b) modified the classic generalized plane strain assumption introduced by Lekhnitskii (1963) to include axial shear and used a 2-D finite element method to analysis axial shear in their problem. Sun and Vaidya (1996) used a 3D finite element method to study the normal, transverse shear and axial shear loading of unidirectional (UD) composites. Inclusion of the thermal residual stress in shear analysis of composite is much more difficult, since the boundary conditions for shear loading are asymmetric, while dose for the prediction of thermal residual stress are symmetric. Nedele and Wisnom (1994) developed a 3-D finite element model using ABAQUS that includes an approximate boundary condition for combination of thermal and shear loading conditions.

Micromechanical modeling of the off-axis loading in practical has received relatively little attention. Aboudi

*Corresponding author, Assistant Professor
E-mail: i_ahmadi@znu.ac.ir

(1988, 1989) used his analytical micromechanical model to predict the strength of a unidirectional composite under complex loading. Foye (1973) developed a finite element micromechanical model for composite laminate subjected to a general combination of normal and shear stresses. However, details of the boundary conditions which are used for combination of shear and normal loading were not provided in his work. Aghdam *et al.* (2001) developed a 3D finite element micromechanical model using ANSYS to predict the behavior of unidirectional metal matrix composite subjected to off-axis loading. Zhu and Sun (2003) studied the behavior of AS4/PEEK composite under off-axis loading using a 3D finite element-based micromechanical approach. Zhu *et al.* (1998) used a 3D finite element micromechanical model to analysis biaxial loading and off-axis loading of composite materials and to predict the strength of a unidirectional composite under complex loading conditions. Carvelli and Corigliano (2004) studied the transverse strength of long-fiber composites and considering perfect bonded and perfect de-bonded fiber-matrix interface. Totry *et al.* (2008) studied the failure of C/PEEK composites in transverse comparison and axial shear loading using computational micromechanics. Sirivedin *et al.* (2007) used the micromechanical model and Elasto-plastic finite element (FE) analysis to study the effects of thermal residual stress in the damage of cross-ply carbon fiber/epoxy composite. Vaughan and McCarthy (2011) studied the micromechanics of fibrous composite and found out that in case of a strong fiber-matrix interface, thermal residual stresses improve the transverse tensile strength. Melro *et al.* (2013) developed micromechanical damage model suitable for epoxy matrix material which accounts for different behavior under transverse tension, transverse compression, and longitudinal and transverse shear.

Moncada *et al.* (2012) used the generalized method of cells to study progressive damage in composites. Sayyidmousavi *et al.* (2014) used a micromechanical approach to study the fatigue failure of unidirectional polymer matrix composites subject to off-axis loading. Erfani and Akrami (2016) used the micromechanical fatigue model to evaluate the cyclic fracture in perforated beams. Hassanzadeh-Aghdam *et al.* (2015) developed a 3D micromechanics-based analytical model to investigate the influence of interphase on the thermo-mechanical properties of three-phase composites. Rohwer (2015) studied the different models on failure and damage of composite materials employing different failure theories. Aghayei *et al.* (2015) studied the different failure criteria to predict the damage in glass/polyester composite materials.

As mentioned before, researchers used analytical approaches and FE modeling to predict the behavior of composite material in off-axis loading and to predict the failure behavior of composites in micromechanical points of view. Recently, meshless methods have become very attractive and efficient for solving boundary value problems. In the meshless methods, nodes can be easily added and removed without need for re-meshing of elements. Various meshless methods are developed by different authors in two last decades. For example one can

refer to diffuse element method (Nayroles *et al.* 1992), Element Free Galerkin (EFG) method (Belytschko *et al.* 1994), reproducing kernel particle method (Liu *et al.* 1996), meshless local Petrov-Galerkin (MLPG) method (Atluri and Zhu 1998) and meshless finite mixture (MFM) method (Cheng *et al.* 2004). Some applications of the meshless methods in the literature include the solution of elasto-static/dynamic problems (Atluri and Zhu (2000), Long *et al.* 2006), plate bending (Gu and Liu 2001, Belinha and Dinis 2006, Sladek *et al.* 2007, Kanok-Nukulchai *et al.* 2001), fracture mechanics (Belytschko and Gu 1995, Ching and Batra 2001), Navier-Stokes flow (Atluri and Shen 2002) and micromechanics of composite materials (Dang and Sankar 2008, Ahmadi and Aghdam 2010 a,b).

To the knowledge of authors, the analysis of off-axis loading of composite materials using 2D-generalized plane strain method, which reduces the computational cost, is not found in the literature. On the other hand, the available papers in open literature used 3D finite element modeling to model the RVE of UD composite subjected to off-axis, axial-transverse and thermal loading conditions. In this study, a modified generalized plane strain micromechanical model is developed to study the combination of transverse and axial normal, shear and thermal loading of fibrous composites in order to model the off-axis and biaxial loading of the composite. This model is employed to study the biaxial and off-axis loading of SiC/Ti and Kevlar/Epoxy composite in the presence of the effects of the thermal residual stresses. A truly meshless method is developed to solve the governing equation of the problem over the RVE. The RVE includes a fiber surrounded in the matrix as repeating element of square array packing of fiber. A perfect connection is considered between fiber and matrix, and displacement continuity and traction reciprocity conditions satisfied in the fiber matrix interface. A failure criterion is considered for the fiber-matrix interface failure. The transverse-transverse, axial-transverse and off-axis loading of SiC/Ti and Kevlar/Epoxy composite are investigated. Quadratic (Von Misses) and Maximum stress failure criteria are considered for prediction the failure in the fiber and matrix. The failure envelopes of the composite are investigated with Direct Micromechanical Model (DMM) and compared with those of phenomenological criteria, such as Tsai-Hill criteria.

2. Modeling

2.1 Off-axis loading

Consider a unidirectional fiber reinforced composite with parallel aligned fibers in the x_1 direction as shown in Fig. 1. The tension load is applied to the composite in Z direction so that the fibers are aligned at angle θ with respect to the loading direction, Z . The spatial coordinate system XYZ as shown in Fig. 1 is defined so that Z -axis aligned in the loading direction and Y -axis shows the thickness direction of the specimen and fibers are aligned in the XZ plane. The material principle coordinate system $x_1x_2x_3$, is defined so that x_3 aligned in the fiber direction and

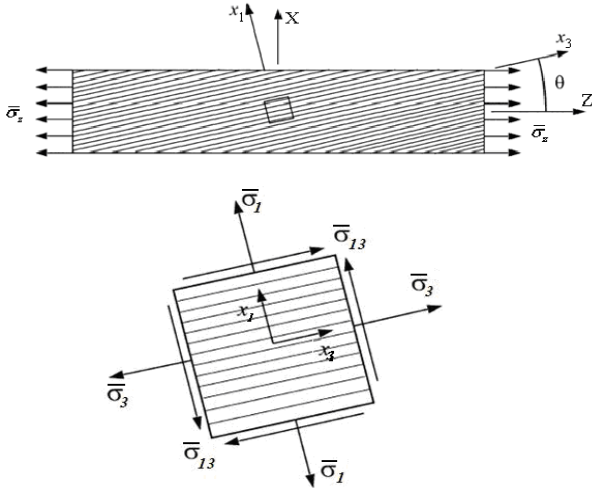


Fig. 1 Off-axis loading of composite material, and stress components in principle coordinates of the composite

x_2 axis coincides with the Y -axis. The composite is subjected to known off-axis tension load in the Z direction and the average stress in the loading direction is $\bar{\sigma}_z$. The symbol $\bar{\sigma}$ indicates the average macro-stress which is applied to a sufficiently large volume of the composite.

In the case of off-axis loading as shown in Fig. 1, the stress state within the specimen in the material principle coordinate $x_1x_2x_3$, consists of three stress components and can be obtained as

$$\begin{aligned}\bar{\sigma}_1 &= \frac{\bar{\sigma}_z}{2}(1 - \cos 2\theta), \\ \bar{\sigma}_3 &= \frac{\bar{\sigma}_z}{2}(1 + \cos 2\theta), \\ \bar{\sigma}_{13} &= -\frac{\bar{\sigma}_z}{2}\sin 2\theta\end{aligned}\quad (1)$$

in which $\bar{\sigma}_3$ is the macro normal stress in the fiber direction, $\bar{\sigma}_1$ is the transverse macro stress and $\bar{\sigma}_{13}$ is the axial shear stress and θ is the angle between the fiber direction and the loading direction as indicated in Fig. 1. So the micromechanical model for analysis of the off-axis loading of UD composite must be able to consider combined axial and transverse normal loading and axial shear loading of the composite.

2.2 Micromechanical modeling of composites

In the micromechanical modeling of unidirectional fibrous composites, in order to simplify the model and reduce the computational cost, usually the actual distribution of the fibers within the cross-section of the composite is simplified to regular and periodic array of fibers in the matrix. In the present study, fibers are assumed to have circular cross section and arranged in the square array fiber packing. In this case, the smallest repeating area of the composite is chosen as the Representative Volume Element (RVE) or unit cell. In general, modeling the off-

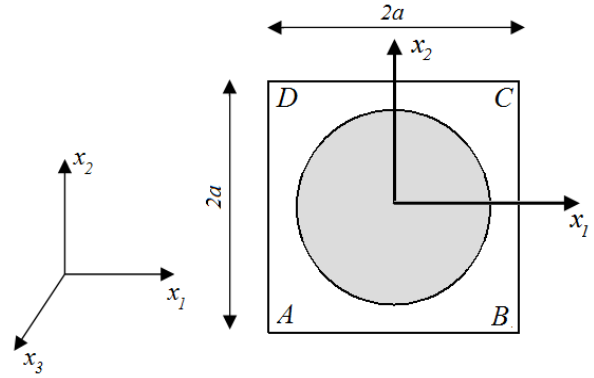


Fig. 2 Selected Representative Volume Element (RVE) and the coordinate system

axis loading conditions which includes combination of axial and transverse normal load and axial shear load requires a 3-D representative volume element. Modeling and analysis of such RVE computationally is expensive. In this study, in order to reduce the computational cost, the generalized plane strain (GPS) model of Lekhnitskii (1963) is used for modeling of the problem. In GPS assumption of the RVE, the strain field is invariant along the fiber axis, x_3 , i.e., $\varepsilon = \varepsilon(x_1, x_2)$ and the normal strain in the fiber, x_3 direction is constant as ε_0 . This treatment allows displacements to occur in all three coordinate directions, but each displacement is dependent upon the x_1 - and x_2 -coordinate, i.e., $u_1 = u_1(x_1, x_2)$, $u_2 = u_2(x_1, x_2)$ and the displacement in the x_3 -direction has an added linear dependence on the x_3 -coordinate, i.e., $u_3 = \varepsilon_0 x_3 + w_3(x_1, x_2)$ where u_1 , u_2 and u_3 are the displacements in the x_1 , x_2 and x_3 directions, respectively and ε_0 is unknown constant strain in the fiber, x_3 direction. In this case, a 2-dimensional RVE as shown in Fig. 2 can be chosen which reduces the computational cost of the solution. It is clear that the employed GPS model considered all six components of strain, but the strain field is invariant along the fiber, x_3 -axis, so the stress field in the RVE is independent from the x_3 coordinate.

2.3 Boundary and Interface conditions

In the micromechanical analysis of the RVE, proper consideration must be given to the periodicity and symmetry of the model in arriving at the correct boundary conditions for different loading situations. Under longitudinal and transverse normal loading, a typical RVE deforms in such a way that it remains a right parallelepiped, i.e., plane sections remain plane. In general, because the composite materials can be envisaged as a periodical array of the RVEs, therefore, the periodic boundary conditions must be applied to the RVE. This implies that each RVE in the composite has the same deformation mode and there is no separation or overlap between the neighboring RVEs. The periodicity conditions of displacements on the boundary of the RVE can be expressed as

$$u_i(\mathbf{x} + \mathbf{d}) - u_i(\mathbf{x}) = \bar{\varepsilon}_{ij} d_j \quad (2)$$

In which \mathbf{d} is the micro-structural scale of the RVE,

which defines the distance from a point \mathbf{x} on the boundary of the RVE to its mirror point on the opposite boundary and $\bar{\varepsilon}_{ij}$ is the average macroscopic strains. It can be seen that although the difference of the displacements for the corresponding points on the two opposite boundary surfaces are specified, the individual displacement component is still a function of the coordinates, i.e., a plane does not necessarily remain a plane after the deformation. For example, according to (3), the periodic boundary conditions for u_i and w component of displacements can be written as

$$\begin{aligned} u_1(a, x_2) - u_1(-a, x_2) &= 2a\bar{\varepsilon}_{11} \\ u_1(x_1, b) - u_1(x_1, -b) &= 2b\bar{\varepsilon}_{12} \\ w_3(a, x_2) - w_3(-a, x_2) &= 2a\bar{\varepsilon}_{11} \\ w_3(x_1, b) - w_3(x_1, -b) &= 2b\bar{\varepsilon}_{12} \end{aligned} \quad (3)$$

In which $2a$ and $2b$ are the length and the width of the RVE, respectively. The traction boundary conditions on the faces of the RVE must be considered as

$$\begin{aligned} T_i(a, x_2) &= -T_i(-a, x_2) \\ T_i(x_1, b) &= -T_i(x_1, -b) \end{aligned} \quad (4)$$

On the other hand, the following relation can be written between the applied macro-stresses which are applied to the TVE and the micro-stresses

$$\begin{aligned} \int_{x_2=-b}^{x_2=b} \sigma_1 dx_2 &= 2b\bar{\sigma}_1 & \int_{x_1=-a}^{x_1=a} \sigma_{12} dx_2 &= 2a\bar{\sigma}_{12} \\ \int_{x_1=-a}^{x_1=a} \sigma_2 dx_1 &= 2a\bar{\sigma}_2 & \int_{x_2=-b}^{x_2=b} \sigma_{13} dx_2 &= 2b\bar{\sigma}_{13} \\ \iint_{\Omega} \sigma_3 dx_1 dx_2 &= (4ab)\bar{\sigma}_3 & \int_{x_1=-a}^{x_1=a} \sigma_{23} dx_2 &= 2a\bar{\sigma}_{23} \end{aligned} \quad (5)$$

In which $\bar{\sigma}$ denotes the external macro-stress applied to the RVE and can be obtained in (1). For fully bonded fiber-matrix interface, the continuity of displacement and reciprocity of traction in the fiber-matrix interface must be satisfied.

3. Meshless formulation

In this study a meshless formulation based on the MLPG method (Atluri and Shen 2002) is employed for solution of the problem. For a continuum body with the domain Ω which is in the static equilibrium, all of the sub-particles Ω_s^l that are located inside the body is in the equilibrium conditions. Ignoring the body force, the equilibrium equation in the weak form for a sub-particle (sub-domain) Ω_s^l inside Ω can be written as

$$\int_{\Omega_s^l} \sigma_{ij,j} w dV = \int_{\Omega_s^l} (\sigma_{ij} w)_{,j} dV - \int_{\Omega_s^l} \sigma_{ij} w_{,j} dV = 0, \quad i = 1, 2, 3 \quad (6)$$

where w is the weight function in the Petrov-Galerkin method. Using the divergence theorem, the above equation can be written as

$$\int_{\partial\Omega_s^l} t_i w dV - \int_{\Omega_s^l} \sigma_{ij} w_{,j} dV = 0, \quad i = 1, 2, 3 \quad (7)$$

where $t_i = \sigma_{ij} n_j$ is the traction vector on the boundary of the sub-domain and $\partial\Omega_s^l$ is the boundary of the local sub-domain. Generally, $\partial\Omega_s^l$ contain three parts, L_s^l is the part which is located totally inside the global domain and Γ_{st}^l and Γ_{su}^l are parts of $\partial\Omega_s^l$ that coincide with the global traction and the global essential boundary, respectively. In the Petrov-Galerkin method, w is an arbitrary function and can be chosen so that it vanishes on L_s^l . By this integration on L_s^l vanishes and Eq. (7) can be written as

$$\int_{\Omega_s^l} \sigma_{ij} w_{,j} dV - \int_{\Gamma_{su}^l} t_i w d\Gamma = \int_{\Gamma_{st}^l} \bar{t}_i w d\Gamma, \quad i = 1, 2, 3 \quad (8)$$

The second and third terms of Eq. (8) vanish for the subdomains that totally are located inside the global domain.

4. Solution of problem

According to (1), the off-axis loading of the RVE consists of combination of axial and transverse normal loading, and axial shear loading of the RVE. In isotropic fiber and matrix, the shear stresses are not coupled with normal strains and with transverse normal and shear stresses. The axial shear component of the loading i.e., $\bar{\sigma}_{13}$ causes only axial shear strains in the x_3 direction i.e., ε_{13} in the RVE.

4.1 Governing equations

According to the displacement field of GPS, it is clear that the strains and stresses are uniform in the x_3 direction and so it is clear that $\sigma_{ij,3} = 0$. In this case the equilibrium equations in the x_1, x_2 and x_3 direction can be written as

$$\begin{aligned} \sigma_{11,1} + \sigma_{12,2} &= 0 \\ \sigma_{12,1} + \sigma_{22,2} &= 0 \\ \sigma_{13,1} + \sigma_{23,2} &= 0 \end{aligned} \quad (9)$$

As seen, the x_3 coordinate is eliminated. For isotropic materials, the first and second equations of (9) are coupled differential equations on $u_1(x_1, x_2)$ and $u_2(x_1, x_2)$ and the third equation is a differential equation on $w_3(x_1, x_2)$. Using (8), the weak form of Eq. (9) in the matrix form can be written as

$$\int_{\Omega_s^l} \bar{\mathbf{B}} \boldsymbol{\sigma} dA - \int_{\Gamma_{su}^l} \mathbf{W} \mathbf{t} d\Gamma = \int_{\Gamma_{st}^l} \mathbf{W} \bar{\mathbf{t}} d\Gamma \quad (10)$$

in which $\bar{\mathbf{B}}$ and \mathbf{W} are defined as

$$\bar{\mathbf{B}} = \begin{bmatrix} w_{,1} & 0 & 0 & 0 & w_{,2} \\ 0 & w_{,2} & 0 & 0 & w_{,2} \\ 0 & 0 & w_{,2} & w_{,2} & 0 \end{bmatrix} \quad (11)$$

$$\mathbf{W} = \{w(x_1, x_2) \quad w(x_1, x_2) \quad w(x_1, x_2)\}^T$$

in which $w(x_1, x_2)$ are weight function and $\boldsymbol{\sigma}$ and \mathbf{t} are defined as

$$\begin{aligned}\boldsymbol{\sigma} &= \{\sigma_{11} \ \sigma_{22} \ \sigma_{23} \ \sigma_{13} \ \sigma_{12}\}^T \\ \mathbf{t} &= \{t_1 \ t_2 \ t_3\}^T\end{aligned}\quad (12)$$

The axial strain ε_0 is unknown constant and must be obtained in the problem solution. ε_0 is written separately in the matrix form of stress-strain relations, and the stress-strain relation for each constituent in the RVE in the presence of temperature change ΔT can be written as

$$\boldsymbol{\sigma} = \mathbf{C}\boldsymbol{\varepsilon} + \mathbf{C}_0\varepsilon_0 - \mathbf{C}_T\Delta T \quad (13)$$

where $\boldsymbol{\sigma}$ is defined in (12) and according to the displacement field, $\boldsymbol{\varepsilon}$ can be written as

$$\begin{aligned}\boldsymbol{\varepsilon} &= \{\varepsilon_{11} \ \varepsilon_{22} \ 2\varepsilon_{23} \ 2\varepsilon_{13} \ 2\varepsilon_{12}\}^T = \\ &= \{u_{1,1} \ u_{2,2} \ w_{3,2} \ w_{3,2} \ u_{1,2} + u_{2,1}\}^T\end{aligned}\quad (14)$$

where the matrix \mathbf{C} , \mathbf{C}_0 and \mathbf{C}_T are defined as

$$\begin{aligned}\mathbf{C} &= \begin{bmatrix} C_{11} & C_{12} & 0 & 0 & 0 \\ C_{12} & C_{22} & 0 & 0 & 0 \\ 0 & 0 & C_{44} & 0 & 0 \\ 0 & 0 & 0 & C_{55} & 0 \\ 0 & 0 & 0 & 0 & C_{66} \end{bmatrix}, \mathbf{C}_0 = \begin{bmatrix} C_{13} \\ C_{23} \\ 0 \\ 0 \\ 0 \end{bmatrix}, \\ \mathbf{C}_T &= \begin{bmatrix} C_{11}\alpha_1 + C_{12}\alpha_2 + C_{13}\alpha_3 \\ C_{12}\alpha_1 + C_{22}\alpha_2 + C_{23}\alpha_3 \\ 0 \\ 0 \\ 0 \end{bmatrix}\end{aligned}\quad (15)$$

The subdomains are located in the x_1x_2 plane and the outward normal to the surface of the subdomains is $\mathbf{n}=(n_1, n_2, 0)$, so the traction on the boundary of the subdomains can be obtained as

$$\mathbf{t} = \{t_1 \ t_2 \ t_3\}^T = \mathbf{N}\boldsymbol{\sigma} \quad (16)$$

where

$$\mathbf{N} = \begin{bmatrix} n_1 & 0 & 0 & 0 & n_2 \\ 0 & n_2 & 0 & 0 & n_1 \\ 0 & 0 & n_2 & n_1 & 0 \end{bmatrix} \quad (17)$$

4.2 Discretization of equations

In order to discretize the equations, a kind of approximation method is needed. One of the well-known methods for approximation of the field variable $u(\mathbf{x})$ over a number of randomly located nodes within the solution domain is the moving least squares (MLS) technique which is described in Atluri and Shen (2002). In this method the nodal interpolation of $u(\mathbf{x})$ is expressed as

$$u^h(\mathbf{x}) = \sum_{J=1}^N \phi^J(\mathbf{x}) \hat{u}^J \quad \mathbf{x} \in \Omega_{\mathbf{x}} \quad (18)$$

where $\phi^J(\mathbf{x})$ is called the shape function of the MLS approximation corresponding to node J and \hat{u}^J are

fictitious nodal values of the field variable. More details on construction of the shape functions can be found in Atluri and Shen (2002).

Using the MLS discretization approach, the strains $\boldsymbol{\varepsilon}$ which are defined in (14) can be written in the discretized form as

$$\boldsymbol{\varepsilon} = \sum_J^N \mathbf{B}^J \hat{\mathbf{u}}^J \quad (19)$$

in which dummy index means summation from 1 to N , and

$$\mathbf{B}^J = \begin{bmatrix} \phi_{,1}^J & 0 & 0 \\ 0 & \phi_{,2}^J & 0 \\ 0 & 0 & \phi_{,2}^J \\ 0 & 0 & \phi_{,1}^J \\ \phi_{,2}^J & \phi_{,1}^J & \phi_{,2}^J \end{bmatrix}, \quad \mathbf{u} = \begin{Bmatrix} \hat{u}_1 \\ \hat{u}_1 \\ \hat{w}_3 \end{Bmatrix} \quad (20)$$

and $\phi_{,i}^J$ is the partial derivative of $\phi^J(\mathbf{x})$ respect to the x_i . The details for obtaining $\phi_{,i}^J$ can be found in Atluri and Shen (2002). By substituting from (13) and (19) into (10), the governing equation of the problem can be obtained as

$$\begin{aligned}\sum_{J=1}^N \int_{\Omega'_s} \bar{\mathbf{B}}\mathbf{C}\mathbf{B}^J \hat{\mathbf{u}}^J dA - \sum_{J=1}^N \int_{\Gamma'_{su}} \mathbf{W}\mathbf{N}\mathbf{C}\mathbf{B}^J \mathbf{u}^J d\Gamma = \\ \int_{\Gamma'_{st}} \bar{\mathbf{t}} d\Gamma + \varepsilon_0 \left(\int_{\Gamma'_{su}} \mathbf{W}\mathbf{N}\mathbf{C}_0 d\Gamma - \int_{\Omega'_s} \bar{\mathbf{B}}\mathbf{C}_0 d\Gamma \right) \\ + \Delta T \left(\int_{\Omega'_s} \bar{\mathbf{B}}\mathbf{C}_T d\Gamma - \int_{\Gamma'_{su}} \mathbf{W}\mathbf{N}\mathbf{C}_T d\Gamma \right)\end{aligned}\quad (21)$$

The above equations can be written as

$$\mathbf{K}_{\mathbf{U}} \hat{\mathbf{u}} = \mathbf{f}_T \quad (22)$$

where the stiffness and force matrix can be obtained as

$$\begin{aligned}\mathbf{K}_{\mathbf{U}} &= \int_{\Omega'_s} \bar{\mathbf{B}}\mathbf{C}\mathbf{B}^J dA - \int_{\Gamma'_{su}} \mathbf{W}\mathbf{N}\mathbf{C}\mathbf{B}^J d\Gamma \\ \mathbf{f}_T &= \int_{\Gamma'_{st}} \bar{\mathbf{t}} d\Gamma + \varepsilon_0 \left(\int_{\Gamma'_{su}} \mathbf{W}\mathbf{N}\mathbf{C}_0 d\Gamma - \int_{\Omega'_s} \bar{\mathbf{B}}\mathbf{C}_0 dA \right) \\ &+ \Delta T \left(\int_{\Omega'_s} \bar{\mathbf{B}}\mathbf{C}_T dA - \int_{\Gamma'_{su}} \mathbf{W}\mathbf{N}\mathbf{C}_T d\Gamma \right)\end{aligned}\quad (23)$$

4.3 Imposing the boundary and interface conditions

One of the challenges of meshless methods is imposing the essential boundary conditions and material discontinuity in the problem solution. In this study, the periodic boundary conditions are directly imposed to the global stiffness and force matrices. For example, in the transverse loading one of the periodic boundary conditions on the right and left edges of the RVE is prescribed as

$$u_1(a, x_2) - u_1(-a, x_2) = 2a\bar{\varepsilon}_{11} \quad (24)$$

Eq. (24) can be enforced to the nodes that are located on right and left edges of the RVE using MLS approximation as

Table 1 Elastic and thermo-elastic properties of SiC, Ti, Kevlar and Epoxy in the composite system

| Material | E (GPa) | ν | α ($10^{-6}/^{\circ}\text{C}$) | Yield Strength, Y (MPa) |
|-----------|-----------|-------|---|---------------------------|
| SiC Fiber | 409 | 0.2 | 4.5 | 3496 |
| Ti Matrix | 107 | 0.35 | 10 | 910 |
| Kevlar | 130 | 0.3 | - | 2800 |
| Epoxy | 3.5 | 0.35 | - | 58 |

$$\sum_{J=1}^N \phi^J(x_{I^R}) \hat{u} - \sum_{J=1}^N \phi^J(x_{I^L}) u_1^J = 2a\bar{\epsilon}_{11} \quad (25)$$

where I^R indicates the node on the right edges of the RVE at (a, x_2) and I^L is the conjugate nodes located on the same point on the left edge of the RVE at $(-a, x_2)$. Eq. (25) is added as a row to the global stiffness and force matrix for the nodes that are located on the boundary. Also the continuity of displacement and reciprocity of traction at the fiber-matrix interface for fully bonded interface must be imposed as

$$\begin{aligned} \mathbf{u}^f - \mathbf{u}^m &= 0 \\ \mathbf{t}^f + \mathbf{t}^m &= 0 \end{aligned} \quad \text{at the interface} \quad (26)$$

in which superscript f and m denotes fiber and matrix, respectively.

5. Numerical results and discussion

In the numerical results, the unidirectional SiC/Ti and Kevlar/Epoxy composite are studied. It is assumed that fibers have circular cross sections and arranged at the square array in the matrix. The Representative Volume Element (RVE) for the composite system is taken as Fig. 2. The elastic and thermo-elastic properties and yield strength of fibers and matrixes are considered as Table 1. The failure envelopes of SiC/Ti with 35% FVF and Kevlar/Epoxy with 63% FVF in the biaxial and off-axis loading are investigated in the numerical results. The thermal residual stress and its effects on the failure envelopes of SiC/Ti are considered in the analysis. The results show that the failure envelopes are affected by the thermal residual stress in the composite.

5.1 Interface failure criteria

One of the most important features of metal matrix composites is generally the low strength of the interface between the fibers and matrix. In this study, two failure criteria are considered for fiber-matrix interface.

1- The Maximum Interface Normal Stress criteria which supposed that the tensile normal to interface stress (σ_n) causes the failure of the interface at tension.

2- The Maximum Interface Shear Stress criteria which supposed that the shear stress on the interface (τ) causes the failure of the interface.

It is supposed that shear strength of the interface is affected by the friction between the fiber and matrix. Compressive stress on the interface increases the shear

strength of the interface. The friction depends on the compressive normal stress on the interface. So in the present study the failure criteria of the interface are considered as;

(a) In tension of the interface ($\sigma_n > 0$)

$$\begin{aligned} \sigma_n &\leq Y_n \\ \tau &\leq Y_n \end{aligned} \quad \text{for } \sigma_n > 0 \quad (27)$$

(b) In compression of the interface

$$\tau \leq Y_n - \mu\sigma_n \quad \text{for } \sigma_n < 0 \quad (28)$$

where Y_n is the strength of the interface in normal tension and supposed to be $Y_n = 55$ MPa (Li and Wisnom 1996) and μ is a factor that shows the dependency of shear strength of the interface to the compressive normal stress on the interface. In (27) and (28), σ_n is the normal to interface stress and τ is the shear stress on the fiber interface. It is supposed that the fiber-matrix interface does not fail by normal compressive stress.

5.2 Strength prediction of composite using direct micromechanics

In this section the presented micromechanical model is applied to predict the strength of SiC/Ti composite and Kevlar/Epoxy composite though prediction of the micro-stresses in the fiber, matrix and fiber-matrix interface for axial and transverse loading. The failure may begin to occur in the fiber, matrix or interface due to the micro-stresses. Prediction of the failure of the composite based on the analysis of micro-stresses in the fiber, matrix and interface is named direct micromechanical model (DMM). Various failure criteria can be considered for predicting the failure in the fiber and in the matrix. For example the Maximum stress criteria or the Quadratic (Von Misses) criteria may be employed to predict the failure initiation in the fiber or matrix. Also interface failure criteria may be considered in prediction the Failure of the RVE. The Maximum stress criteria are usually used for brittle materials such as ceramics and Quadratic criteria are usually used for ductile materials such as metals. For abbreviation of failure criteria, the letter Q is used to refer to Quadratic (Von Misses) criteria and M is used to denote Maximum normal stress criteria.

In this study, a two letter notation such as AB is used to illustrate the combinations of the failure criteria which are employed to predict failure in the fiber and matrix. The first letter, A denotes the criteria that are used for predicting of failure in the fiber and the second one, B stands for the criteria which are used for prediction of failure in the matrix in the composite system. For example notation QM means that the Quadratic criterion is used for fiber, Maximum normal stress criteria is used for matrix and interface failure is not considered for fiber-matrix interface and QQ means that Quadratic criteria is employed for both fiber and matrix and interface failure is not considered. The predicted strength of the RVE based on failure of the interface (Interface Normal Stress and Interface Shear Stress) is reported separately in the tables and figures. The failure

Table 2 Predicted Strength Values of SiC/Ti with 35% FVF with DMM without considering the thermal residual stress, $Y_n=55$ MPa (the most conservative value in each column is bolded)

| Criteria | X_T (GPa) | X_C (GPa) | Y_T (GPa) | Y_C (GPa) | S_{13} (GPa) | S_{12} (GPa) |
|---|---------------|---------------|---------------|---------------|----------------|----------------|
| QQ | 1.8103 | 1.8103 | 0.7833 | 0.7833 | 0.3712 | 0.5078 |
| MQ | 1.8103 | 1.8103 | 0.7833 | 0.7833 | 0.3712 | 0.5078 |
| QM | 1.7721 | 1.7721 | 0.6592 | 0.6592 | 0.6445 | 0.8471 |
| MM | 1.7721 | 1.7721 | 0.6592 | 0.6592 | 0.6445 | 0.8471 |
| Interface failure (Max. Interface Normal stress) | - | 2.1913 | 0.0413 | 0.3561 | - | 0.0524 |
| Interface failure, (Max. Interface Shear Stress, $\mu=0.8$) | - | 9.6862 | 0.0971 | 0.1457 | 0.0387 | 0.0455 |
| The most conservative values (Composite Strengths) | 1.7721 | 1.7203 | 0.0413 | 0.1457 | 0.0387 | 0.0455 |

Table 3 Predicted Strength of Kevlar/Epoxy with 63% FVF with DMM without considering thermal residual stress

| Criteria | $X_T=X_C$ (MPa) | $Y_T=Y_C$ (MPa) | S_{13} (MPa) | S_{12} (GPa) |
|----------|-----------------|-----------------|----------------|----------------|
| QQ | 1377 | 51 | 17.5 | 20.7 |
| MQ | 1377 | 51 | 17.5 | 20.7 |
| QM | 1340 | 29 | 15.1 | 17.9 |
| MM | 1340 | 29 | 15.1 | 17.9 |

strength of the fibers and matrix are shown in Table 1. The interface bonding strength between the fiber and matrix is supposed to be $Y_n=55$ MPa (Li and Wisnom 1996). In this study the results are presented for $Y_n=55$ MPa, 300 MPa and 500 MPa.

5.2.1 Uniaxial strength

The strengths of the SiC/Ti and Kevlar/Epoxy composite in uniaxial normal and shear loading are studied based on the analysis of the RVE. This type of analysis is named direct micromechanical method (DMM). The predicted strength values of SiC/Ti composite without considering the thermal residual stress (TRS) are shown in Table 2. In this table, X_T and X_C refer to the tensile and compressive strength composite in the axial direction and Y_T and Y_C refer to the tensile and compressive strength in the transverse direction, respectively and S refers to the shear strength of the composite. The predicted results based on the combination of different criteria are tabulated in Table 2. A look at Table 2 makes it clear that same value for X_T as 1.7721 GPa is predicted for SiC/Ti by MQ and MM criteria which this value is more conservative than QQ and QM criteria in predicting the axial strength of SiC/Ti. The QQ and QM criteria also predicts same value for axial tensile strength as $X_T=1.8103$ GPa. In the prediction of X_T , because the results of MQ and MM are the same and the results of QQ and QM are the same, so it is concluded that fiber controls the failure initiation of SiC/Ti in the axial loading and maximum stress criteria (M) is more conservative. In axial tensile loading of SiC/Ti composite, the normal stress at the interface (σ_n) is compressive and so the interface will not fail in the axial tension.

In Table 2, the predicted value for transverse strength of SiC/Ti is $Y_T=41.3$ MPa and $Y_C=145.7$ MPa and is obtained by Interface Normal Stress and Interface Shear Stress

criteria. So the dominant failure mode for axial loading is failure of fiber, the dominant mode for transverse tensile loading is Interface Normal Stress criteria and the dominant failure mode for transverse compressive loading is interface shear stress criteria.

The unidirectional strengths of unidirectional Kevlar/Epoxy composite with 63% FVF which are obtained by the micromechanical model using different failure criteria for matrix and fiber are shown in Table 3.

The fiber-matrix failure criteria are not considered for Kevlar/Epoxy composite. The table includes the transverse normal Y , axial normal Y and shear strength S_{12} and S_{13} . It is seen that the predicted strengths of Kevlar/Epoxy composite do not depend on the chosen failure criteria of Fiber. The predictions of QQ are the same as MQ, and the predictions of QM are the same as MM. It means that matrix control the failure of the Kevlar/Epoxy composite.

The strengths of the SiC/Ti composite with considering the thermal residual stress (TRS) are shown in Table 4. It must be noted that the manufacturing process of SiC/Ti metal matrix composite takes place at the temperature about 910°C and after manufacturing, the composite is cooled down to the room temperature. Because of the mismatch in the coefficient of thermal expansion of the fiber and matrix the change of temperature will cause serious thermal residual stresses in the composite at the room temperature. To estimate the thermal residual stress in the SiC/Ti composite system, it is assumed that the composite system is stress free at the manufacturing temperature and during the cooling the thermal residual stresses arise in the composite. For prediction of the thermal residual stresses in SiC/Ti, it is supposed that the composite components are stress free in the manufacturing temperature 910°C, so at the room temperature (25°C) the composite system is subjected to decrease in temperature as $\Delta T=25-910=-885$ °C. Due to this temperature change a compressive thermal residual stress about -300MPa will occur at the fiber-matrix interface on x_1 axis in radial direction. Also the axial thermal residual stress at fiber is about -810 Mpa and in the matrix on x_1 axis is about 420 MPa.

It can be seen that in the presence of TRS the axial strength of SiC/Ti is reduced. It is seen in Table 4 that in the presence of TRS, axial tension strength (X_T) is not affected by the failure criteria of the fiber. So it can be claimed that by considering the residual stresses, tension strength in fiber

Table 4 Predicted Strength values of SiC/Ti with 35% FVF with DMM in presence of thermal residual stress, $Y_n=55$ MPa

| Criteria | X_T (GPa) | X_C (GPa) | Y_T (GPa) | Y_C (GPa) | S_{13} (GPa) | S_{12} (GPa) |
|--|---------------|---------------|--------------|---------------|----------------|----------------|
| QQ | 0.3307 | 1.5084 | 0.3252 | 0.1020 | 0.1611 | 0.2219 |
| MQ | 0.3307 | 1.4080 | 0.3252 | 0.1020 | 0.1611 | 0.2219 |
| QM | 0.8226 | 1.5084 | 0.5356 | 0.4354 | 0.5574 | 0.6446 |
| MM | 0.8226 | 1.4080 | 0.5356 | 0.4354 | 0.5574 | 0.6446 |
| Interface failure, (Max. Interface Normal Stress) | - | - | 0.277 | 2.4868 | - | 0.1585 |
| Interface failure, (Max. Interface Shear Stress, $\mu=0.8$) | - | - | 0.1366 | 0.8380 | 0.1585 | 0.1057 |
| The most conservative values (Composite Strengths) | 0.3328 | 1.4080 | 0.277 | 0.1020 | 0.1585 | 0.1057 |

direction (X_T) is controlled by failure of matrix. It is due to the fact that axial thermal residual stress in the matrix is tensile and about 410 MPa. Also based on Table 3, it can be concluded that the axial strength of composite in compression (X_C) is controlled by failure of fiber because as seen in Fig. 5, the axial thermal residual stress is compressive in the fiber (about -790 MPa). Because of the large value of compressive residual stress in the fiber, in the axial compression of SiC/Ti, fibers fail before matrix.

Table 5 shows that by considering the thermal residual stress and using the Interface Normal Stress criteria, the transverse strength of SiC/Ti is predicted as $Y_T=277$ MPa. The experiment value for the transverse failure initiation of SiC/Ti is reported about 250 MPa by Li and Wisnom (1996) and Nimmer *et al.* (1991). So, it is concluded that predictions of the Interface Normal Stress criteria is more close to the experiment data. The Interface Normal Stress criteria are selected as interface failure criteria in most of the presented figures in the next sections.

The predicted transverse strength of composite is increased by considering the thermal residual stress (TRS). This is due to the compressive TRS in the fiber-matrix interface. Hu (1996) reported the experimental data for initiation of de-bonding for a single fiber material as 247 MPa. They predicted the residual stress in the interface as 321 MPa.

5.2.2 Biaxial transverse-transverse loading

The composite system which is subjected to state of biaxial stress in the transverse directions x_1 and x_2 is considered. The external normal stresses $\bar{\sigma}_1$ and $\bar{\sigma}_2$ are the only nonzero external loads that are applied to the composite. The direct micromechanical method (DMM) is used to predict the failure envelopes of composite in transverse-transverse loading.

The failure envelopes of the SiC/Ti composite in transverse-transverse loading, without considering the thermal residual stresses are shown in Fig. 3. This figure contains the envelopes obtained by micromechanical approach for the case of QQ, MQ, QM and MM. In Fig. 3, it is clear that QQ and MQ criteria predict the same envelopes and QM and MM predict the same envelopes. It means that failure of matrix controls the failure of the RVE in transverse-transverse loading. The figure contains the failure envelope predicted by phenomenological Tsai-Hill

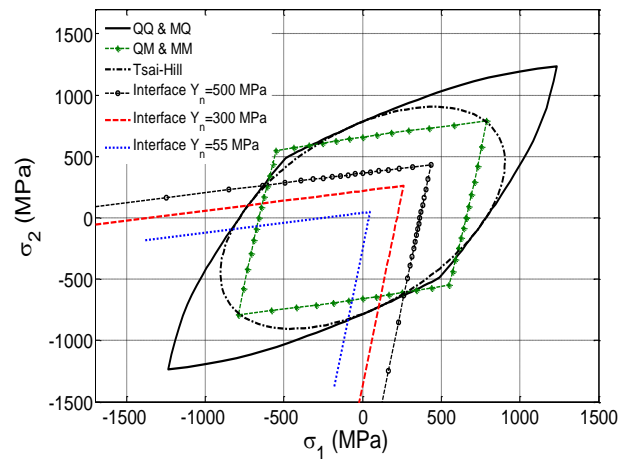


Fig. 3 Failure envelopes of SiC/Ti in transverse-transverse loading without considering the thermal residual stress

criteria. The Tsai-Hill envelope is obtained based on the uniaxial strengths of the RVE which are obtained by QQ criteria in Table 2. Also the predictions obtained by Interface Normal Stress criteria by $Y_n=500$ MPa, 200 MPa and 55 MPa are included in Fig. 3. Based on Fig. 3, it is obvious that QM and MM are more conservative than QQ and MQ in predicting the failure envelopes. As seen in the figure, because of weak fiber-matrix interface, in the absence of the thermal residual stress, the transverse tensile strength of the composite which are predicted based on the failure of interface has very small value.

The failure envelopes of SiC/Ti composite in $(\bar{\sigma}_1, \bar{\sigma}_2)$ plane by considering the thermal residual stresses are shown in Fig. 4. The effects of residual stresses on the failure envelopes are seen in this Figure. By comparing Fig. 4 with Fig. 3, it is clear that the failure envelopes in $(\bar{\sigma}_1, \bar{\sigma}_2)$ plane are shifted due to presence of compressive transverse residual stress in the matrix. The compressive residual stress at the fiber-matrix interface tends to delay the fiber-matrix de-bonding in transverse tension. For $Y_n=55$ MPa, based on the interface failure criteria, in the presence of thermal residual stress the strength of composite in uniaxial transverse loading is increased from 41.3 MPa to 277 MPa.

5.2.3 Biaxial axial-transverse loading

The failure envelopes of SiC/Ti composite in Axial-

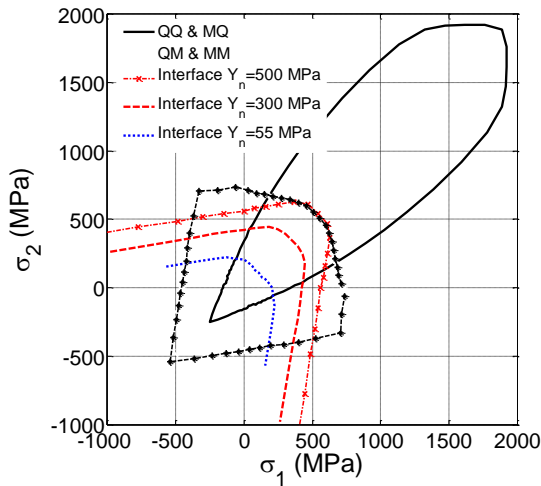


Fig. 4 Failure envelopes of SiC/Ti in transverse-transverse loading in presence of thermal residual stress

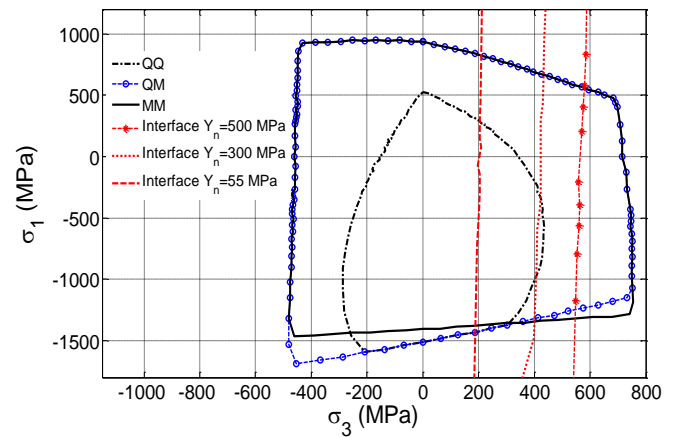


Fig. 6 Failure envelopes of SiC/Ti in axial-transverse loading in presence of thermal residual stress

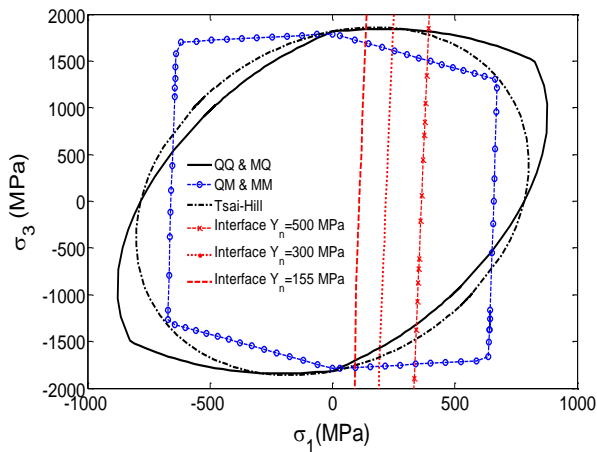


Fig. 5 Failure envelopes of SiC/Ti in axial-transverse loading without considering thermal residual stress

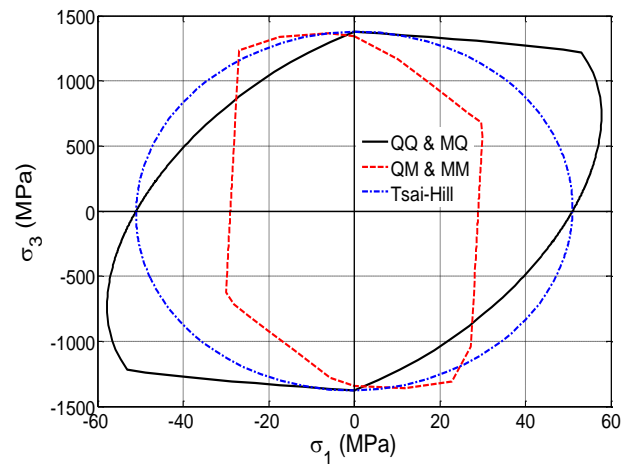


Fig. 7 Failure envelopes of Kevlar/Epoxy composite in axial-transverse loading

Transverse loading in the absence of thermal residual stress are shown in Fig. 5. The envelope for QQ is the same as MQ and envelope for QM is the same as MM. So it can be concluded that matrix is the dominant constituent in failure of SiC/Ti in $(\bar{\sigma}_3, \bar{\sigma}_1)$ plane. For tensile transverse stress ($\sigma_1 > 0$), interface damage controls the failure of composite. For compressive transverse stress ($\sigma_1 < 0$), the interface will not fail and matrix controls the failure of the composite.

The effects of the thermal residual stress on the failure envelopes of SiC/Ti in $(\bar{\sigma}_3, \bar{\sigma}_1)$ plane are shown in Fig. 6. In the presence of the thermal residual stresses the envelopes is shifted to the negative side of axial stress. Shifting the envelope to the negative side of the σ_3 is due to the positive thermal residual stress in the matrix in axial direction. In Fig. 6, it is seen that the dominant failure mode of composite for positive axial loading ($\sigma_3 > 0$) is the failure of matrix and for negative axial stress ($\sigma_3 < 0$) is the failure of fiber. Because the thermal residual stress in the fiber is compressive, in the presence of thermal residual stress the axial strength of the composite is decreased in axial compression.

The failure envelopes of Kevlar/Epoxy composite with 63% FVF in Axial-Transverse loading of the composite with different failure criteria are shown in Fig. 7. It is seen that the failure criteria which is used for the fiber has no effect on the failure envelopes of the Kevlar/Epoxy composite and failure of the matrix is dominant in the failure envelopes of the composite.

5.2.4 Off-axis loading

Off-axis loading of SiC/Ti and Kevlar/Epoxy composite is simulated in this section. Fig. 8 indicates the failure curve for off-axis loading of the SiC/Ti composite without considering the effect of thermal residual stress for $\theta = 0$ to 90° . The failure curves for MQ (QQ) and MM (MN) are shown in this figure. Two criteria for fiber-matrix interface failure are considered in this figure:

a) Interface Normal Stress criterion; which means that the normal to fiber-matrix interface stress causes debonding of interface.

b) Interface Shear Stress criterion; which means that the shear stress on the interface causes the failure of interface.

The off-axis failure curves for SiC/Ti are presented for $Y_n = 300$ MPa and $Y_n = 55$ MPa. It is seen in Fig. 8 that for

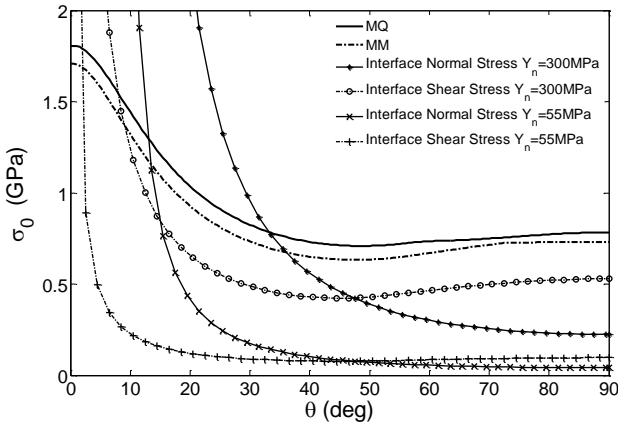


Fig. 8 Failure curve for SiC/Ti in off-axis loading with various failure criteria, without considering thermal residual stress

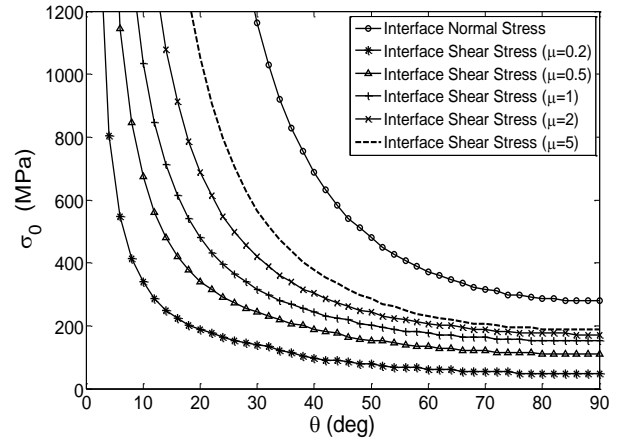


Fig. 9 Failure curve of SiC/Ti in off-axis loading in presence of thermal residual stress

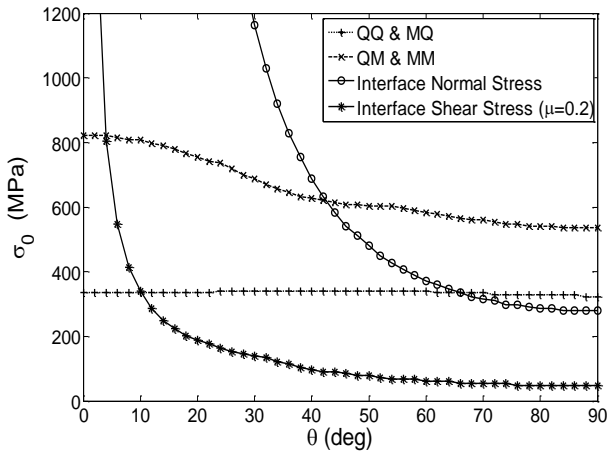


Fig. 9 Failure curve of SiC/Ti in off-axis loading in presence of thermal residual stress

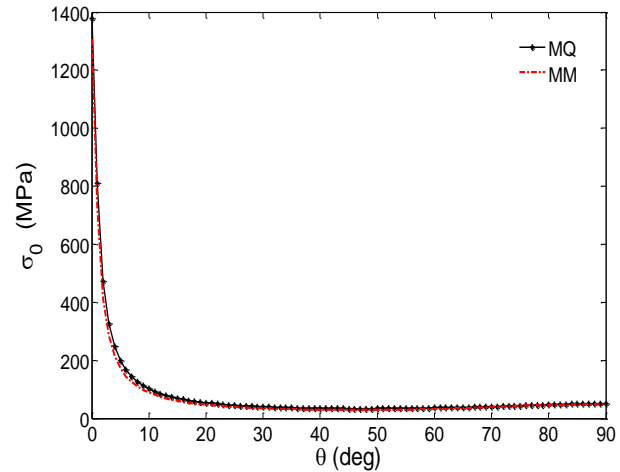


Fig. 11 Off-axis failure curve of Kevlar/Epoxy composite with MQ and MM failure criteria

$Y_n=55$ MPa, the Interface Shear Stress criteria for $2.5^\circ \leq \theta \leq 48^\circ$ is more conservative than the Interface Normal Stress criterion and is the dominant criteria in failure of SiC/Ti in off-axis loading. For $48^\circ \leq \theta \leq 90^\circ$ the Interface Normal Stress is most conservative. For $Y_n=300$ MPa, Interface Shear Stress is the dominant criteria for $8^\circ \leq \theta \leq 48^\circ$ and Interface Normal Stress criterion is dominant for $\theta > 48^\circ$.

The off-axis strength curves of SiC/Ti with considering the thermal residual stress are shown in Fig. 9. It is seen in Fig. 9 that the QQ (and MQN) has the most conservative predictions for $\theta > 18^\circ$. The failure of interface based on Interface Normal Stress and Interface shear stress ($\mu=0.2$) are shown in this figure. Fig. 9 shows that the axial strength is decreased and transverse strength is increased in the presence of thermal residual stresses. The experimental data shows that the transverse tensile strength for SiC/Ti is about 250 MPa (Li and Wisnom 1996). The Interface Normal Stress criterion predicts the value about 277 MPa for transverse failure initiation. The residual stress in Ti in axial direction is tensile and about 410 MPa. This tensile stress decreased the axial tensile strength of the composite.

The effect of μ on the interface failure curve of SiC/Ti in off-axis loading is shown in Fig. 10. It is clear in Fig. 10

that the strength of SiC/Ti in off-axis loading is increased by increasing the value of μ .

The off-axis failure curves of Kevlar/Epoxy composite are shown in Fig. 11. This figure shows the prediction of the micromechanical modeling for the strength of the Kevlar/Epoxy composite by MQ and MM criteria. The results of QQ criteria is the same as MQ and the results of QM is the same as MM. Thermal residual stress and interface damage are not considered in these diagrams.

6. Conclusions

In this paper, a general micromechanical model is developed to study the behavior of unidirectional composite which is subjected to combination of biaxial, thermal and off-axis loading conditions. In order to avoid full 3D modeling of RVE, the modified generalized plane strain assumption is employed for modeling the 3D state of loading of composite. The direct micromechanical method (DMM) is used to predict the micro-stresses in the composite system in order to obtain the failure envelopes of the composite in the biaxial and off-axis loading conditions.

Combinations of failure criteria are used for fiber, matrix and fiber-matrix interface in composite system. SiC/Ti and Kevlar/Epoxy composite are studied. The induced thermal residual stress in the manufacturing process of SiC/Ti is considered and its effects on the failure envelopes is investigated. In the presence of thermal residual stress, the transverse-transverse failure envelopes are shifted to the positive side of transverse stresses and the axial-transverse failure envelopes are shifted to the negative side of the axial stress. Comparison of the predicted results of the present model with experimental data shows excellent agreement. The failure initiation envelopes which are obtained by the direct micromechanical method (DMM) are compared with the envelope obtained by the phenomenological Tsai-Hill criteria. Direct micromechanical method is also used for prediction of yield strength of SiC/Ti in the axial and transverse direction. It is shown that the interface failure is the dominant failure mode for most cases of loading.

References

- Aboudi, J. (1988), "Micro-mechanical analysis of the strength of unidirectional fibre composites", *Compos. Sci. Technol.*, **33**, 79-96.
- Aboudi, J. (1989), "Micro-mechanical analysis of composites by the method of cells", *Appl. Mech. Rev.*, **42**, 193-221.
- Adams, D.F. (1970), "Inelastic analysis of a unidirectional composite subjected to transverse normal loading". *J. Compos. Mater.*, **4**, 310-328.
- Adams, D.F. and Crane, D.A. (1984), "Combined loading micromechanical analysis of a unidirectional composite", *Compos.*, **15**(3), 181-192.
- Adams, D.F. and Crane, D.A. (1984), "Finite element micromechanical analysis of a unidirectional composite including longitudinal shear loading", *Comput. Struct.*, **18**(6), 1153-1165.
- Adams, D.F. and Doner, D.R. (1967), "Transverse normal loading of a unidirectional composite", *J. Compos. Mater.*, **1**, 152-164.
- Aghaei, M., Forouzan M.R., Nikforouz, M. and Shahabi, E. (2015), "A study on different failure criteria to predict damage in glass/polyester composite beams under low velocity impact", *Steel Compos. Struct.*, **18**(5), 2015
- Aghdam, M.M, Pavier, M.J. and Smith, D.J. (2001), "Micro-mechanics of off-axis loading of fibrous composites using finite element analysis", *Int. J. Solid. Struct.*, **38**(22), 3905-3925.
- Aghdam, M.M., Smith, D.J. and Pavier, M.J. (2000), "Finite element micro-mechanical modeling of yield and collapse behaviour of metal matrix composites", *J. Mech. Phys. Solid.*, **48**(3), 499-528.
- Ahmadi, I. and Aghdam, M.M. (2010a), "Micromechanics of fibrous composites subjected to combined shear and thermal loading using a truly meshless method", *Comput. Mech.*, **64**(3), 387-398.
- Ahmadi, I. and Aghdam, M.M. (2010b), "Analysis of micro-stresses in the SiC/Ti metal matrix composite using a truly local meshless method", *Proc. Inst. Mech. Eng., Part C: J. Mech. Eng. Sci.*, **224**(8), 1567-1577.
- Atluri, S.N. and Shen, S. (2002), *The Meshless Local Petrov-Galerkin (MLPG) Method*, Tech Science Press.
- Atluri, S.N. and Zhu, T. (1998), "A new meshless local Petrov-Galerkin (MLPG) approach in computational mechanics", *Comput. Mech.*, **22**, 117-127.
- Atluri, S.N. and Zhu, T. (2000), "The meshless local Petrov-Galerkin (MLPG) approach for solving problems in elastostatics", *Comput. Mech.*, **25**, 169-179.
- Belinha, J. and Dinis, L.M.J.S. (2006), "Analysis of plates and laminates using the element-free Galerkin method", *Comput. Struct.*, **84**, 1547-1559.
- Belytschko, T., Lu, Y.Y. and Gu, L. (1995), "Crack Propagation by Element Free Galerkin Methods", *Eng. Fract. Mech.*, **51**(2), 211-222.
- Belytschko, T., Lu, Y.Y. and Gu, L. (1994), "Element-free Galerkin methods", *Int. J. Numer. Meth. Eng.*, **37**, 229-256.
- Brockenbrough, J.R., Suresh, S. and Wienecke, H.A. (1991), "Deformation of metal-matrix composites with continuous fibers: Geometrical effects of fiber distribution and shape", *Acta Metall. Mater.*, **5**, 735-752.
- Carvelli, V. and Corigliano, A. (2004), "Transverse resistance of long-fibre composites: influence of the fibre-matrix interface", *Proceedings of the 11th European conference on composite materials ECCM11*, Rhodes, Greece, May-June.
- Cheng, J.Q. Lee, H.P. and Li, H. (2004), "Development of a meshless finite mixture (MFM) method", *Struct. Eng. Mech.*, **17**(5), 671-690.
- Ching, H.K. and Batra, R.C. (2001), "Determination of crack tip fields in linear elastostatics by the meshless local Petrov-Galerkin (MLPG) method", *CMES: Comput. Model. Eng. Sci.*, **2**(2), 273-290.
- Cooper, G.A. (1966), "Orientation effects in fibre-reinforced metals", *J. Mech. Phys. Solid.*, **14**, 103-111.
- Dang, T.D. and Sankar, B.V. (2008), "Meshless local Petrov-Galerkin micromechanical analysis of periodic composites including shear loadings", *CMES: Comput. Model. Eng. Sci.*, **26**(3), 169-187.
- Dvorak, G.J., Rao, M.S.M. and Tarn, J.Q. (1973), "Yielding in unidirectional Composites under external loads and temperature changes", *J. Compos. Mater.*, **7**, 194-216.
- Erfani, S. and Akrami, V. (2016), "Evaluation of cyclic fracture in perforated beams using micromechanical fatigue model", *Struct. Eng. Mech.*, **20**(4), 913-930.
- Foy, R.L. (1973) "Theoretical post-yielding behaviour of composite laminates part I- Inelastic micromechanics", *J. Compos. Mater.*, **7**, 179-193.
- Gu, Y.T. and Liu, G.R. (2001), "A meshless local Petrov-Galerkin (MLPG) formulation for static and free vibration analysis of thin plates", *CMES: Comput. Model. Eng. Sci.*, **2**(4), 463-476.
- Hassanzadeh-Aghdam, M.K., Mahmoodi, M.J. and Ansari, R. (2015), "Interphase effects on the thermo-mechanical properties of three-phase composites", *Proc. Inst. Mech. Eng., Part C: J. Mech. Eng. Sci.*, **230**(19), 3361-3371.
- Hu, S. (1996), "The transverse failure of a single-fiber metal-matrix composite: Experiment and modeling", *Compos. Sci. Technol.*, **56**, 667-676
- Jackson, P.W. and Cratchley, D. (1966), "The effect of fibre orientation on the tensile strength of fibre-reinforced metals", *J. Mech. Phys. Solid.*, **14**, 49-64.
- Kanok-Nukulchai, W., Barry, W.J. and Saran-Yasoontorn, K. (2001), "Meshless formulation for shear-locking free bending elements", *Struct. Eng. Mech.*, **11**(2), 123-132.
- Lekhnitskii, S.G. (1963), *Theory of Elasticity of an Anisotropic Elastic Body*, Holden Day Inc., San Francisco. (English translation from Russian)
- Li, D.S. and Wisnom, M.R. (1996), "Micromechanical modeling of SCS-6 fiber reinforced Ti-6Al-4V under transverse tension-effect of fiber coating", *Comput. Mater.*, **30**(5), 561-88.
- Liu, W.K., Chen, Y., Chang, C.T. and Belytschko, T. (1996), "Advances in multiple scale kernel particle methods", *Comput. Mech.*, **18**, 73-111.
- Long, S.Y., Liu, K.Y. and Hu, D.A. (2006), "A new meshless method based on MLPG for elastic dynamic problems", *Eng. Anal. Bound. Elem.*, **30**, 43-48.

- Melro, A.R., Camanho, P.P., Andrade, Pires, F.M. and Pinho, S.T. (2013), "Micromechanical analysis of polymer composites reinforced by unidirectional fibres: Part II-micromechanical analyses", *Int. J. Solid. Struct.*, **50**, 1906-1915.
- Moncada, A.M., Chattopadhyay, A., Bednarczyk, B.A. and Arnold, S.M. (2012), "Micromechanics-based progressive failure analysis of composite laminates using different constituent failure theories", *J. Reinf. Plast. Compos.*, **21**, 1467-1487.
- Naik, R.A. and Crews, Jr J.H. (1993), "Micromechanical analysis of fiber-matrix interface stresses under thermomechanical loadings", *Composite Materials: Testing and Design (Vol. II), ASTM STP 1206, American Society for Testing and Materials, Philadelphia, PA*, 205-219.
- Nayroles, B., Touzot, B. and Villon, P. (1992), "Generalizing the finite element method: diffuse approximation and diffuse elements", *Comput. Mech.*, **10**, 307-318.
- Nedele, M.R. and Wisnom, M.R. (1994), "Finite element micromechanical modeling of a unidirectional composite subjected to axial shear loading", *Compos.*, **25**(44), 263-272.
- Nimmer, R.P. (1990), "Fibre-matrix interface effects in the presence of thermally induced residual stress", *J. Compos. Tech. Res. JCTRER*, **12**(2), 65-75.
- Nimmer, R.P., Bankert, R.J., Russell, E.S., Smith, G.A. and Wright, P.K. (1991), "Micromechanical modeling of fiber/matrix interface effects in transversely loaded SiC/Ti-6-4 metal matrix composites", *J. Compos. Tech. Res. JCTRER*, **13**(1), 3-13.
- Pipes, R.B. and Cole, B.W. (1973), "On the off-axis strength test for anisotropic materials", *J. Compos. Mater.*, **7**, 246-256.
- Rohwer, K. (2015), "Predicting fiber composite damage and failure", *J. Compos. Mater.*, **49**(21), 2673-2683.
- Sayyidmousavia, A., Bougheraraa, H. and Fawaz, Z. (2014), "A micromechanical approach for the fatigue failure prediction of unidirectional polymer matrix composites in off-axis loading including the effect of viscoelasticity", *Adv. Compos. Mater.*, **24**, 65-77.
- Sirivedin, S., Han, S.Y. and Lee, K.S. (2007), "Micromechanics analysis of progressive failure in cross-ply carbon fiber/epoxy composite under uniaxial loading", *J. Mech. Sci. Technol.*, **21**(12), 2023-2030.
- Sladek, J., Sladek, V., Krivacek, J., Wen, P.H. and Zhang, Ch. (2007), "Meshless local Petrov-Galerkin (MLPG) method for Reissner-Mindlin plates under dynamic load", *Comput. Meth. Appl. Mech. Eng.*, **196**, 2681-2691.
- Sun, C.T. and Vaidya, R.S. (1996) "Prediction of composite properties from a representative volume element", *Compos. Sci. Tech.*, **56**, 171-179.
- Totry, E., González, C. and LLorca, J. (2008), "Prediction of the failure locus of C/PEEK composites under transverse compression and longitudinal shear through computational micromechanics", *Compos. Sci. Tech.*, **68**(15-16), 3128-3136.
- Vaughan, T.J. and McCarthy, C.T. (2011), "Micromechanical modeling of the transverse damage behaviour in fibre reinforced composites", *Compos. Sci. Tech.*, **71**, 388-396.
- Wisnom, M.R. (1990), "Factors affecting the transverse tensile strength of unidirectional continuous Silicon Carbide fibre reinforced 6061Aluminum", *J. Compos Mater.*, **24**(7), 707-726.
- Zahl, D.B., Schmauder, S. and McMeeking, R.M. (1994), "Transverse strength of metal matrix composites reinforced with strongly bonded continuous in regular arrangements", *Acta Metallurgica et Materialia*, **42**(9), 2983-2997.
- Zhu, C. and Sun, C.T. (2003), "Micromechanical modeling of fiber composites under off-axis loading", *J. Thermoplas. Compos. Mater.*, **16**, 333-344.